C*is* non-coding genetic variation drives gene expression changes in the *E. coli* and *P. aeruginosa* pangenomes

Bamu F. Damaris[1,2], Matylda Zietek[3], Jelena Erdmann[1], Athanasios Typas[3,4], Susanne Häußler[1,2,5], and Marco Galardini[1,2]

[1] Institute for Molecular Bacteriology, TWINCORE Centre for Experimental and Clinical Infection Research, a joint venture between the Hannover Medical School (MHH) and the Helmholtz Centre for Infection Research (HZI), Hannover, Germany
[2] Cluster of Excellence RESIST (EXC 2155), Hannover Medical School (MHH), Hannover, Germany
[3] Genome Biology Unit, European Molecular Biology Laboratory (EMBL), Heidelberg, Germany
[4] Molecular Systems Biology Unit, EMBL, Heidelberg, Germany
[5] Department of Clinical Microbiology, Copenhagen University Hospital - Rigshospitalet, Copenhagen, Denmark

Abstract

Bacteria use gene regulation to dynamically adapt to changes in their environment, including resistance to stress and the occupation of new niches. Gene expression is known to vary within a species pangenome, but the extent to which these changes could be explained by genetic variants in *cis* non-coding regions has so far been poorly investigated. Statistical genetics offers a hypothesis-free approach to this problem, as opposed to mechanistic models, which can be used only for reference isolates that are not representative of the whole species. In this study, we assembled two genomic and transcriptomic datasets for *Escherichia coli* (N=117) and *Pseudomonas aeruginosa* (N=413) and identified associations between genetic variants in *cis* non-coding regions and recorded gene expression variation. We identified at least one associated variant in up to 39% of the tested genes in both species. We partly validated the associations *in-silico* and *in-vitro* for *E. coli*, reinforcing the difficulty of identifying a single mechanism generating gene expression diversity. We then investigated the relevance of non-coding variants in explaining the variability in antimicrobial resistance in both species using two additional publicly available datasets, identifying a large number of these variants across antimicrobial compounds. This work confirms the role of genetic variation in often overlooked regions of bacterial genomes in influencing molecular and clinically relevant phenotypes.

Introduction

Population genetics principles[1], harsh competition, and the generally limited resource settings faced by prokaryotes suggest that microbial cells will manage their resources efficiently, therefore tending to express some of their genes only when necessary for survival[2]. Examples of this general principle have been known in the *E. coli* carbon metabolism since the early days of molecular microbiology[3]. This principle also applies to survival to stresses, such as antimicrobial resistance (AMR), as well as occupying new ecological niches, such as the human host for pathogenic species[4].

The same efficiency principle results in physically interacting and functionally related genes being encoded in operons, usually controlled by a single promoter. The expression of whole functional units encoded in a prokaryotic cell could then largely depend on regulatory elements located in the non-coding region immediately upstream of an operon (*cis* regulation). These non-coding regions contain regulatory elements such as canonical promoters recognized by specific sigma-factors (σ) of the RNA-polymerase, as well as transcription factor binding sites (TFBS) that determine the binding of transcription factors, which in turn favour (activators) or repress (repressors) gene expression[5]. These non-coding regions have in fact been shown to be under selection, suggesting that they are evolutionarily constrained because of the impact that mutations in these regions could ultimately have on survival[6,7]. Given the high plasticity of bacterial genomes, genetic variants in non-coding regions can take up multiple forms, each of which may alter gene expression. Short variants such as SNPs/InDels have been shown to be able to create active promoter sequences from random sequences when put under selection[8]. Larger genetic variants such as promoter switching enable genes to be wired to a different section of the regulatory network, thus enabling phenotypic changes that do not depend on altering the coding sequence[9].

Even though the field of synthetic biology has over the years accumulated knowledge on how to combine the presence of specific regulatory elements to achieve the desired level of expression, how much natural genetic variation influences observed variations across different bacterial isolates is currently unknown. Although non-coding regions only account for 10-15% of a prokaryotic genome on average, the impact of genetic variants in those regions could result in large phenotypic changes, comparable to those observed for variants in coding regions, as well as gene presence/absence patterns. These changes could then affect observable phenotypes such as antimicrobial resistance[10] and pathogenicity[11].

Correctly predicting the impact of non-coding variants on gene expression is a difficult task due to the large number of regulatory elements contributing to the outcome and how they interact with each other, not all of which have been studied. Detailed biophysical models and large scale library screens have been able to improve the understanding of the relationship between primary sequences and corresponding gene expression levels[12,13], but these are limited to the reference laboratory isolate of *E. coli*, and cannot be used to generalize to natural isolates and across genes and species.

In this study we set out to identify non-coding genetic variants affecting gene expression in a collection of *E. coli* and *Pseudomonas aeruginosa* isolates, for which we obtained both genomic and transcriptomic data. We used a statistical genetics approach that does not rely on prior knowledge of regulatory elements, and only used the assumption that genetic variants affecting gene expression would be located in non-coding regions located in *cis*. In order to capture all sources of genetic variation affecting gene expression levels, we encoded genetic variants using traditional short variants (SNPs/InDels), promoter switching, and gene cluster k-mers[14].

78 We could find at least one *cis* genetic variant associated with gene expression across isolates
79 for up to 39% of the genes we tested (713 genes for *E. coli* and 1,632 genes in *P. aeruginosa*),
80 some of which we validated experimentally and could mechanistically explain in *E. coli* thanks
81 to the detailed knowledge of its canonical promoter structure and TFBS sequence motifs. We
82 then showed how antimicrobial resistance is associated with non-coding variants in both
83 species, and validated it using transcriptomics under tobramycin treatment. Our study
84 provides an approach for identifying genetic variants affecting gene expression and resulting
85 phenotypes in ever larger genomic and transcriptomic bacterial collections.

Results

Natural and clinical isolates of *E. coli* and *P. aeruginosa* exhibit distinct gene expression profiles compared to reference strains

In this study we aimed to map the role of *cis* non-coding genetic variants in the regulation of gene expression in *E. coli* and *P. aeruginosa*, using an hypothesis-free approach. We analyzed transcriptomic profiles in rich media and genomic data from 117 *E. coli* and 413 *P. aeruginosa* isolates (**Figure 1**). The *E. coli* isolates were mostly clinical (45%) and natural isolates (30%), with lab strains (5%) and experimental evolution isolates (20%) being the minority. The *P. aeruginosa* isolates were all clinical isolates. We measured the transcriptomes of *E. coli* as part of this study, and obtained transcriptomic information for *P. aeruginosa* isolates from a previous study[10,15]. Through a differential gene expression analysis between each isolate and their respective reference genome we revealed significant differences in gene expression among the isolates. To account for differences in gene presence/absence patterns in the species' pangenome, we defined differentially expressed genes (DEGs) as those present in at least 10% of isolates, with an absolute $\log_2$ fold-change ≥ 2 in at least 5% of isolates, and an adjusted p-value < 0.0001.

In *E. coli*, we identified 713 DEGs accounting for 17% of the K-12 proteome. A sizable portion of these genes were those associated with virulence (19%) and antimicrobial resistance (14%). Most of these genes (66%) were a part of operons with diverse biological functions (**Supplementary Table 1**). For example, all genes within the *fimAICDFGH* operon were differentially expressed. This operon encodes type I fimbriae, which facilitates bacterial adhesion and invasion of host tissues[16]. Similarly, within the *acrAB* operon, *acrB* alone was differentially expressed across strains. This operon encodes for part of the AcrAB/TolC multidrug efflux pump, which contributes to antimicrobial resistance, as well as adaptation to the host intestinal environment by exporting bile salts and enabling bacterial survival in host immune cells[17]. We then performed a functional enrichment analysis on the DEGs, which revealed an enrichment of two major COG (cluster of orthologous groups) categories (**Figure 1C**): cell motility and translation, and ribosomal structure and biogenesis. With the key genes in the cell mobility category being *fliC*, which encodes flagellin protein essential for flagellar filaments, *motA* and *motB*, which are necessary for motor rotation[18]. For the translation and ribosomal structure category, notable genes included *hchA*, a stress-response gene[18].

Since we had transcriptomic data for more *P. aeruginosa* strains, we uncovered more than double of DEGs (1,632), corresponding to 27% of the PA14 reference proteome. Among these, 10% were associated with virulence, and 4% associated with antimicrobial resistance. A substantial proportion of the DEGs (25%) were part of an operon, many of which contributed to bacterial survival and adaptability (**Supplementary Table 2**). For instance, three of the six genes in the alginate biosynthesis operon (*alg44KEGXL*), which regulates alginate biosynthesis[19], were differentially expressed. Four out of seven genes in the *pelABCDEFG* operon, which encode polysaccharides critical for environmental persistence and biofilm formation[20], were differentially expressed. Another operon of note was *flgBCDE*, where two out of four genes were differentially expressed. This operon plays a central role in flagellar assembly and motility[21]. Several DEGs, including *mexAB-oprM*, *mexXY*, and *mexCD-oprJ*, were identified in operons associated with multidrug resistance[22]. The DEGs were enriched in several functional categories (**Figure 1D**), including intracellular trafficking, secretion, and vesicular transport. Key genes in this category include *exbB2*, transmembrane proteins, and *pilQ*/*pilC*, which are essential for the assembly of a type IV pilus[23]. Another prominent category was translation, ribosomal structure, and biogenesis, represented by genes such as *rpmJ* (50s ribosomal protein L36), *rpsT* (30S ribosomal protein S20), and *rplT* (50S ribosomal protein L20)[18].

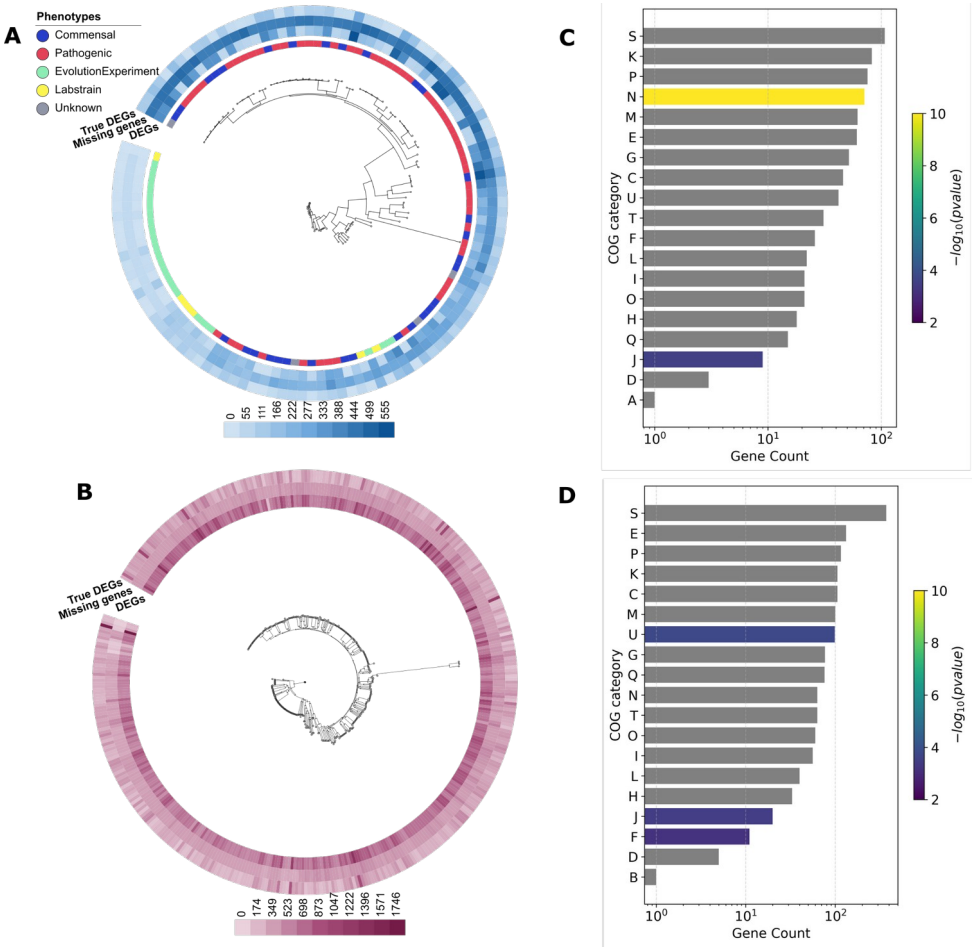

Figure 1: **Variability in gene expression in a panel of *E. coli* and *P. aeruginosa* strains. (A-B)** Phylogenetic trees based on the core genomes of the *E. coli* **(A)** and *P. aeruginosa* **(B)** isolates. The color intensity of the outer rings reflects the gene count within each category. "Missing genes" refers to those absent in the genome of the corresponding isolate in the tree. DEGs are those with an absolute $\log_2$ fold-change ≥ 2 and an adjusted p-value < 0.0001. "True DEGs" are the number of DEGs excluding those that are missing from the genome of the corresponding isolate in the tree. **Panels (C)** and **(D)** illustrate the functional diversity of DEGs in *E. coli* and *P. aeruginosa* isolates, respectively, compared to their reference strains. The horizontal bars represent the number of genes associated with each COG category (**Supplementary Table 3**). The color scale reflects the statistical significance adjusted for multiple testing.

These results highlight the significant transcriptional differences between the isolates and their reference genomes in *E. coli* and *P. aeruginosa*. The observed transcriptional variations are likely driven by genetic variants, some of which might be in *cis* (*i.e.* in direct proximity) with respect to each DEG or operon.

150 **A large fraction of gene expression changes can be attributed to genetic variations in**
151 ***cis* non-coding regions**

152 Next, we used three types of genetic markers to characterise the genetic variants within the *cis*
153 non-coding regions of the DEGs, which were: short variants like single nucleotide
154 polymorphisms (SNPs) and short insertions and deletions (InDels), the presence/absence of
155 intergenic regions (IGRs), and k-mers. By using these different ways of encoding variants, we
156 aimed to compensate for the limitations of each encoding method, to capture a larger fraction
157 of variants, and lastly to improve the interpretation for those variants significantly associated
158 with gene expression changes. We identified a total of 136,690 short variants within the non-
159 coding region of DEGs in *E. coli*, with SNPs comprising the vast majority (85%). Similarly, in *P.*
160 *aeruginosa*, we identified 6,125,235 short non-coding variants in the non-coding region of
161 DEGs, where SNPs accounted for 86% of the total variants. We also analyzed the variability in
162 the presence/absence patterns of entire IGRs. We identified 12,491 IGRs within *E. coli* genes,
163 with 71.6% classified as cloud IGRs, meaning they appeared in 15% or fewer of the genomes
164 analyzed. In *P. aeruginosa*, 22,788 IGRs were identified, with 80.9% being cloud IGRs. A
165 smaller proportion of the core IGRs (found in at least 99% of genomes) was comparable in
166 both species, accounting for 10% in *E. coli* and 10.2% in *P. aeruginosa* (**Supplementary**
167 **Figure 1**).

168 We then conducted a GWAS analysis to establish statistical associations between each
169 gene's *cis* non-coding variants and their corresponding expression. We focused on DEGs that
170 had at least a four-fold expression change when compared to that of the reference strains in ≥
171 5% of isolates, thereby prioritizing genes with significant change of gene expression. We
172 observed that short variants were associated with the expression of 7% of the genes in *E. coli*
173 and 25% in *P. aeruginosa* (**Figure 2**). When measuring associations using IGRs presence or
174 absence within DEGs, we observed that 28% of the DEGs in *E. coli* were linked to IGR
175 variability, whereas this was true only for 3% of DEGs in *P. aeruginosa*. We also observed that
176 k-mers encoding genetic variants, which captures both short variants and IGR
177 presence/absence patterns, improved the sensitivity of our association analysis; in fact we
178 identified significant associations for 39% of the DEGs in both species. The underlying non-
179 coding genetic variants we identified were associated with both upregulated and
180 downregulated gene expression. We observed that when these *cis* short non-coding variants
181 were present in the first gene of an operon, they affected the expression of 6% of downstream
182 genes in the operon in *E. coli* and 35% in *P. aeruginosa*. For both species we have therefore
183 identified significant associations between *cis* variants and changes in gene expression for up
184 to 39% of DEGs. Since promoters and transcription-factor binding sites (TFBSs) are within
185 regions of these *cis*-variants, we reasoned that these elements could at least partially explain
186 these associations.

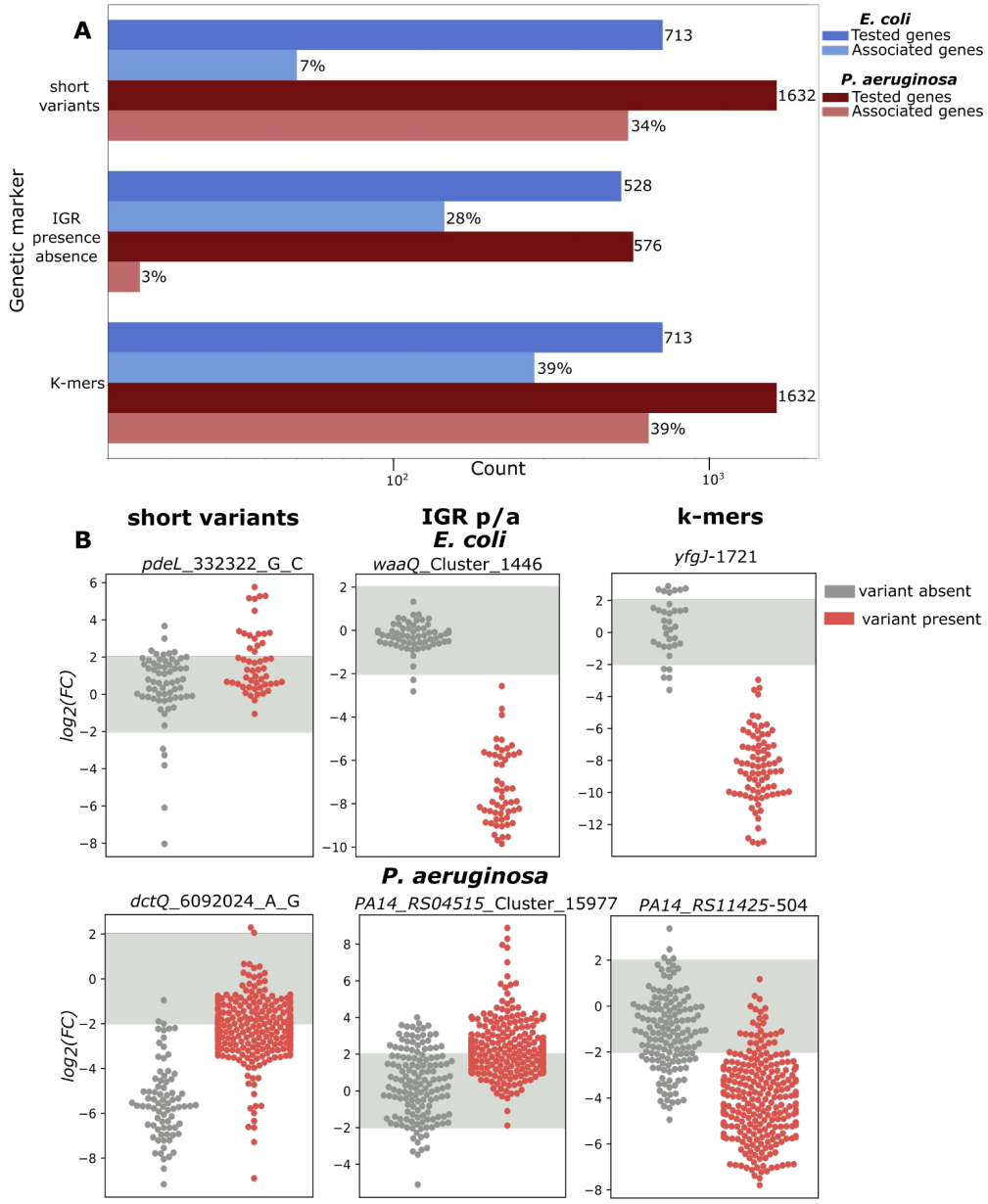

Figure 2: Non-coding variants are associated with gene expression in *E. coli* and *P. aeruginosa*. (A) Summary statistics about the relationship between each genetic marker (short variants, IGR presence/absence, and gene cluster specific k-mers) and gene expression in *E. coli* (blue) and *P. aeruginosa* (maroon). **(B)** Each plot shows fold change for each gene associated with SNPs (left), IGR presence/absence (middle), and gene-clustered k-mers (right). Genes include *pdeL*, *waaQ*, and *yfgJ* in *E. coli*, and *dctQ*, *PA14_RS04515*, and *PA14_RS11425* in *P. aeruginosa*. Each point represents an isolate: grey indicates absence of the non-coding variant, red indicates presence. The grey shaded region marks the differential expression threshold; points (*i.e.* isolates) outside this range are considered to have the gene differentially expressed.

Validation of the effects of non-coding variants on gene expression in *E. coli*

Our association analysis found that variation in gene expression could be explained by the presence of *cis* non-coding variants for up to 39% of DEGs, when encoded using kmers. We then set out to determine the potential mechanism by which these variants exert their effect. We focused these validation approaches for *E. coli*, owing to its well-curated and characterized transcriptional regulatory elements, such as canonical promoters and transcription factors (TFs). To investigate whether non-coding variants previously identified through GWAS are likely to influence gene expression through alterations to canonical promoters, we used a biophysical model[13], which enabled us to predict transcription rates from the variant-containing non-coding sequences. This model specifically estimates transcription rates based on the presence of putative σ^{70} promoters, the primary sigma factor responsible for housekeeping gene expression under standard conditions. We hypothesized that genetic variants present in the site of a canonical promoter could result in altered transcription rates, and that changes in transcription rates would correlate with the measured gene expression. We focused on the 218 DEGs in *E. coli* whose expression levels were significantly associated with non-coding variants, as identified in our k-mer based GWAS. For each gene, we computed the Pearson's correlation coefficient between predicted transcription rates (from the promoter calculator) and measured gene expression across the isolates.

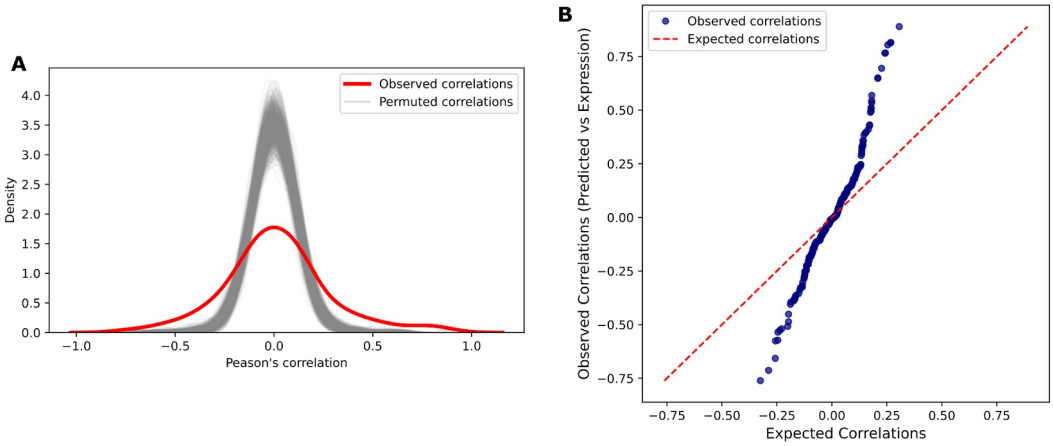

Figure 3: Predicted transcription rates correlate with measured gene expression in *E. coli* isolates. (A) The distribution of observed correlation coefficients (red curve), alongside correlation distribution from individual permutation runs (grey curves), which represent the null distribution generated by shuffling predicted transcription rates for each gene. (**B)** Represents a Q-Q plot comparing observed correlation coefficients (y-axis) to the expected correlation coefficients derived from the permutation tests (x-axis).

We observed that 30% and 3% of DEGs had a moderate ($0.2 < |r| < 0.8$) or strong ($|r| \geq 0.8$) correlation between the predicted transcription rates and the measured gene expression, respectively (**Figure 3A**). We assessed whether these patterns were stronger than what would occur by chance. We performed a permutation, in which the predicted transcription rates were randomly shuffled 1,000 times per gene across isolates and a Pearson's correlation coefficient was computed between them and the measured gene expression values. We observed that the empirical distribution of correlations coefficients differed significantly from the shuffled ones, using a Kolmogorov-Smirnoff test (p-value < 0.0001). A Q-Q plot comparing the observed and expected correlation values further showed enrichment at the tails of the distribution (**Figure 3B**), further supporting the hypothesis that

these DEGs are driven by variants affecting promoters, and that both positive and negative regulatory effects are possible.

While the majority of genes exhibited weak correlations, 17% (N=46) of DEGs demonstrated moderate to strong positive correlations, supporting the hypothesis that these variants can regulate gene expression through their impact on promoters as observed in genes like *yfgJ* (putative oxidoreductase), *kgtP* (α-ketoglutarate transporter), *waaQ* (heptosyltransferase involved in LPS biosynthesis), and *ulaE* (L-ascorbate catabolism enzyme)[24] (**Figure 4**). The remaining unexplained DEGs suggest the presence of additional regulatory mechanisms, either acting in *cis*, or in *trans*.

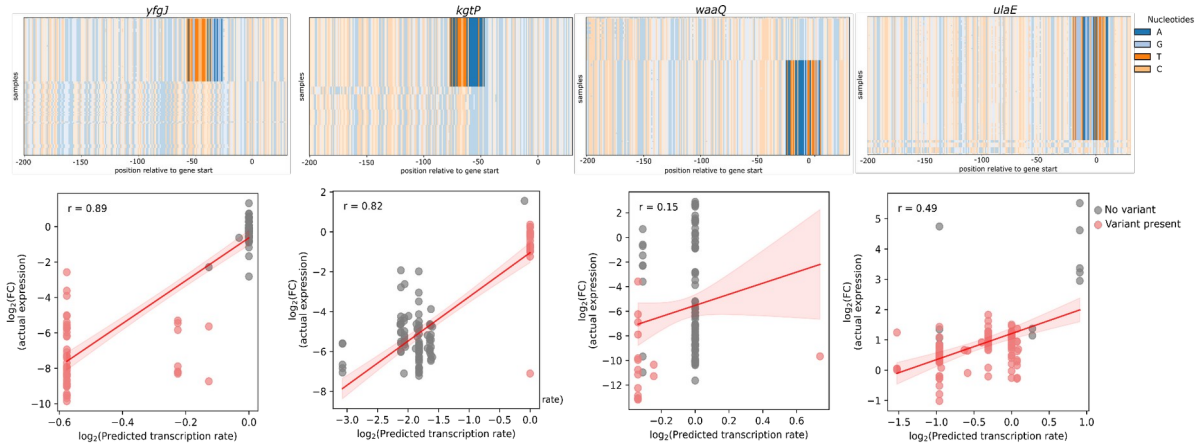

Figure 4: Non coding variants within canonical promoters influence predicted transcription rates and correlate with gene expression. The top panel shows the variant map for four genes (*yfgJ, kgtP, waaQ, ulaE*), with nucleotides aligned relative to the gene's start codon. Solid color regions indicate the non-coding variant altering the predicted transcription rates. Bottom panels show the correlation between the gene's predicted transcription rates and their measured gene expression ($\log_2$ fold change). Isolates with non-coding variants are highlighted in red, and those without the variant are in grey.

Similarly to canonical promoters, transcription factor binding sites (TFBSs) are important sequence-based elements that influence gene expression by allowing for the binding of specific transcription factors (TFs) that can selectively recognize their cognate TFBS and either support (activators) or repress (repressors) transcription. We compiled a list of 93 experimentally validated TFBS motifs from RegulonDB[25] and scanned the non-coding sequences of the DEGs in each *E. coli* isolate to identify the presence or absence of each TF's binding site. We identified the presence of at least one TFBS for 99% of the DEGs (**Supplementary Figure 2**). We then constructed a binary matrix of TFBS presence or absence across isolates and performed a GWAS to evaluate associations between TFBS variation and DEG expression.

We observed significant associations between TFBSs presence and expression for 25% of the tested DEGs (178), of which 129 (72%) had mutated σ^{70} promoters previously identified in our earlier analysis as linked to gene expression. While the presence of TFBS may suggest a potential influence on gene expression, it is important to note that the regulatory effect depends on whether the TF is an activator or repressor. Hence, our observations do not directly correlate with the upregulation or downregulation of the genes. Notably, 5% (23) of the identified TFBSs overlapped with SNP positions previously associated with gene expression. This overlap suggests that these SNPs could potentially alter TF binding by disrupting existing

or creating novel TFBS, which in turn may affect gene transcription and expression, as seen in genes such as *yihM*, *hipB* (antitoxin component of a type II toxin-antitoxin system)[24] (**Figure 5**). Through this second in-silico validation we have identified an additional mechanism driving changes in gene expression through *cis* non-coding genetic variation.

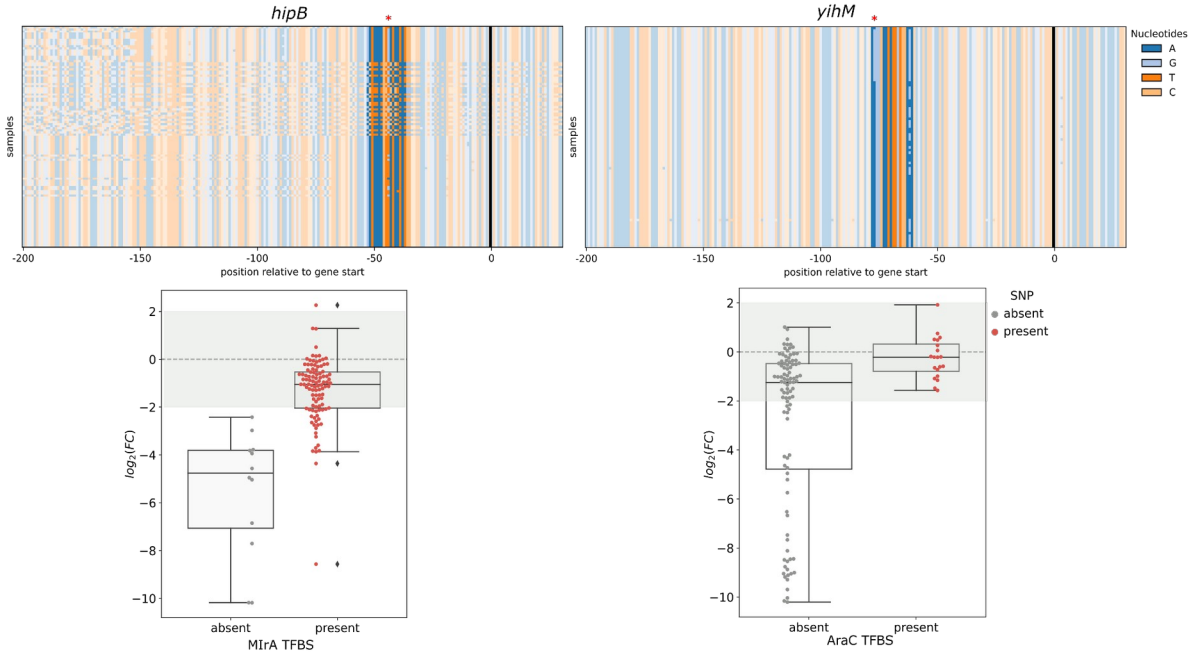

Figure 5: TFBS overlap with SNP positions are significantly associated with altered gene expression in *E. coli*. The top panel represents the variant maps upstream of *hipB* and *yihM* genes, aligned relative to the start codon of the corresponding gene. The red asterisks (*) indicate SNP positions previously linked to gene expression changes and overlap with the TFBS MIrA (for *hipB*) and AraC (for *yihM*). The box plots show the relationship between the SNP presence within the TFBS and gene expression. The y-axis represents log_2 fold changes in expression, while the x-axis indicates the presence or absence of the TFBS. The overlaid swarm plots show the presence (red) or absence (grey) of the variant.

We further validated a selection of the original *E. coli* associations using a fluorescent reporter assay (N=18 genes). We amplified the non-coding regions of these 18 DEGs with significant associations from the reference and from a selected isolate carrying the associated variant, and cloned them upstream of the reporter gene (GFP) into the pOT2 plasmid. Differences in the expression of the GFP gene due to the impact of the variants in gene expression would then translate to differences in observed fluorescence. The generated constructs were cultured in supplemented M9 media, and GFP expression was measured over 16 hours at 30-minute intervals. We observed a clear difference between the GFP expression of the mutated reporter constructs versus those of their wild-type counterparts for 16 genes (**Figure 6A**). Expression changes ranged from -1 to +3-fold, with effect sizes ranging from small (Cohen's $d \leq 0.2$, 2 genes), medium ($0.2 < d < 0.8$, 4 genes), and large effects ($d \geq 0.8$, 12 genes). While the direction of gene expression changes between the reporter fusion assay and the actual gene expression was not always consistent with the original variation measured through RNA-seq, 9 out of 18 genes (50%) showed concordant directionality, which further validates the use of GWAS to find the genetic determinants of gene expression changes.

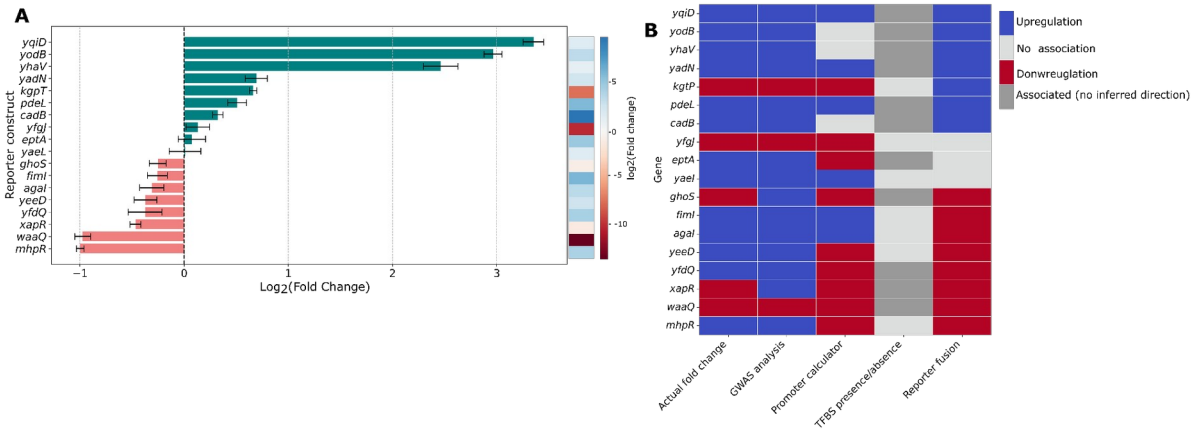

294 **Figure 6: Non-coding variants alter transcription activity in *E. coli*.** Reporter constructs
295 containing either wild-type or mutated non-coding regions were generated for 18 genes.
296 Cultures were grown for 16 hours, with GFP expression measured every 30 minutes.
297 Fluorescence readings were normalized to both blank controls and cell density. To reduce
298 noise observed in early measurements, only data collected after 6 hours were included in the
299 analysis. **(A)** Relative fold-changes in GFP expression of the mutated reporter construct
300 relative to its wild-type counterpart. For each pair, mean fluorescence values were averaged
301 across replicates from the 6-hour time point onwards. Fold enrichment was computed as the
302 ratio of the signal in the mutant to the one in the wild-type. The heatmap on the right shows the
303 fold changes of DEG gene in the initial screen (rich media, exponential growth phase). **(B)**
304 Agreement between the approaches used to establish links between non-coding variants and
305 gene expression changes. The different color indicates the direction of gene expression
306 change associated with each approach. For TFBSs, dark gray indicates a significant
307 association between their presence and gene expression. The direction of the effect cannot be
308 determined, as transcription factors may function as either activators or repressors, and this
309 context-specific role could not reliably be inferred here.

310 We next compared the results from the different approaches used to establish the relationship
311 between non-coding variants and gene expression in *E. coli*: GWAS using k-mers, canonical
312 promoter strength predictions, TFBS presence/absence analysis, and reporter fusion assays
313 (**Figure 6B**). For each method we categorized the predicted effect as upregulation,
314 downregulation, or no significant change. In the GWAS analysis, beta values were used to
315 infer directionality, in the promoter calculator, this was based on the sign of the correlation
316 coefficient between the predicted transcription rates and measured gene expression, and in
317 the reporter assays directionality was inferred based on $\log_2$ fold-change and effect sizes
318 (upregulation with log2 fold-change > 0 and $d \geq 0.5$, downregulation with $\log_2$ fold-change
319 < 0 and $d \geq 0.5$, or no significant change with $d < 0.5$). For TFBS presence/absence
320 however directionality is inherently ambiguous, as the presence of a binding site does not
321 indicate upregulation, nor does its absence imply downregulation. In this context, TFBS
322 associations are best interpreted as indicators of regulatory involvement rather than direct
323 predictors of the direction of expression change. Overall, 22% (N=4, *yqiD*, *pdeL*, *waaQ*, and
324 *yadN*) of the genes showed consistency in their effects on gene expression across all three
325 methods. However, we also observed discrepancies, such as in the case of *ghoS*, where
326 GWAS found an association with upregulation, while the promoter calculator and reporter
327 fusion assays predicted downregulation. Although the TFBS association aligns with higher
328 expression, the unknown role of the TF (activator or repressor) limits functional interpretation
329 (**Figure 6B**). The GWAS analysis showed the highest concordance with the actual gene
330 expression changes, agreeing with observed changes in 89% of cases, which can be expected

as the method uses the actual gene expression to find associations, followed by the promoter calculator which was in agreement in 61% of the cases. The reporter fusion assay and TFBS presence or absence analysis aligned with observed gene changes in 50% of cases. This variability in concordance across genes highlights the multifaceted nature of regulatory control and suggests that no single approach fully captures the complexity of expression variation driven by non-coding genetic variations.

Antimicrobial resistance in *E. coli* and *P. aeruginosa* can be linked to genetic variations within non-coding regions

Antimicrobial resistance (AMR) poses a significant threat to global public health and is driven largely by the genetic adaptability of bacterial pathogens. While the role of protein-coding genes in resistance has been well studied, the contribution of non-coding regulatory regions remains underexplored. We therefore analyzed the genomes of *E. coli* (N=1,675) and *P. aeruginosa* (N=413, the same isolates for which we had available transcriptomic data) isolates, obtained from existing studies[10,26], to understand to what extent non-coding variants can explain antimicrobial resistance in these pathogens.

The *E. coli* isolates were tested for susceptibility against 12 antibiotics including amoxicillin-clavulanic acid (AMC), ampicillin (AMP), cefuroxime (CXM), cefotaxime (CTX), cephalothin (CET), ceftazidime (CAZ), gentamicin (GEN), tobramycin (TOB), ciprofloxacin (CIP), amoxicillin (AMX), trimethoprim (TMP), and piperacillin-tazobactam (TZP). Resistance profiles varied significantly, with AMP showing the highest resistance rate (75% of isolates resistant), while TZP exhibited the highest susceptibility rate (60% of the isolates susceptible) (**Supplementary Fig 3A**). For *P. aeruginosa*, among the four antibiotics, CIP, TOB, CAZ, and meropenem (MEM), tested. TOB showed the highest sensitivity rate (67%) and MEM showed the highest proportion of resistant isolates (74%) (**Supplementary Figure 3B**).

We identified SNPs and InDels within the non-coding regions of these isolates, as previously stated, and conducted a whole-genome GWAS (wGWAS) to identify resistance-associated variants across the genome as well as a *cis*-GWAS focusing only on non-coding variants near genes. Both approaches identified resistance-associated variants in both *E. coli* and *P. aeruginosa* (**Supplementary Figure 4** to **9**).

In *E. coli* the wGWAS and *cis*-GWAS identified on average 137 and 44 genes, respectively, encoding resistance-associated variants across all antibiotics except for amoxicillin (AMX) (**Figure 7A**). The *cis* non-coding variants were found in poorly characterized genes like *yghJ*, *yieH*, and *osmC*, which are implicated in biological processes such as lipoprotein secretion and stress responses and have been previously recognized as markers for predicting AMR in *E. coli*[24]. We also observed that some of the *cis* non-coding variants were similar across different antibiotic classes with the most overlap being between cephalosporins and aminoglycosides (**Figure 7C**). Some variants appeared to play broader roles in resistance across multiple drug classes. For example, non-coding variants in *gadX* were associated with resistance to cephalosporins, aminoglycosides, and fluoroquinolones. GadX is a transcriptional regulator known to enhance expression of the MdtEF efflux pump, which contributes to multidrug resistance[27]. Similarly, non-coding variants in *mbsA*, a homolog of the multidrug resistance ATP-binding cassette (ABC) transporter, were identified in isolates resistant to both cephalosporins and aminoglycosides[28]. This cross-class overlap of non-coding variants suggests their potential role in mediating cross-resistance mechanisms among different antibiotic classes.

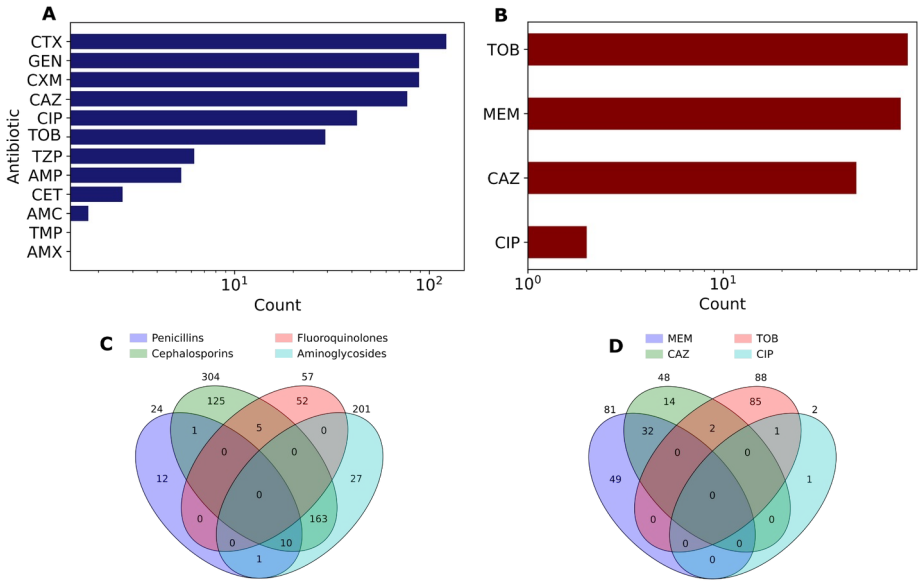

Figure 7: Non-coding variants are associated with antimicrobial resistance in *E. coli* and *P. aeruginosa*. Panels **A)** and **B)** show genes with non-coding variants associated with antibiotic resistance. The y-axis represents the antibiotic and the x-axis represents the number of genes with non-coding variants associated with resistance. **C)** and **D)** represent Venn diagrams that show the overlap and uniqueness of non-coding variants associated with antibiotic resistance across different antibiotics.

In *P. aeruginosa*, we identified on average, 93 genes and 27 genes, for wGWAS and *cis*-GWAS respectively, with resistance-associated variants across all four antibiotics. Among the antibiotics tested, we observed the highest number of genes with resistance-associated non-coding variants for TOB (**Figure 7B**). Some of these non-coding variants were located in the *rpSA* gene which has been linked to translation initiation in *E. coli* and pyrazinamide resistance in *Mycobacterium tuberculosis*[29–31]. However, its specific role in mediating resistance in *P. aeruginosa* remains unclear. We also identified a non-coding variant in the *murU* gene, which encodes N-acetylmuramate α-1-phosphate uridylyltransferase, which is involved in peptidoglycan recycling and has been linked to antibiotic resistance in *P. aeruginosa* through its regulation of cell wall precursor pools[32]. Some of the non-coding variants were shared between CAZ and MEM as well as between TOB and CAZ, suggesting a potential cross-resistance mechanism between these antibiotic classes (**Figure 7D**). This cross resistance could result from overlapping regulatory pathways that influence resistance to these different antibiotics.

Non-coding variants confer tobramycin resistance by affecting bacterial cell wall and outer membrane composition

We identified a SNP in *E. coli*, a T>C transition, at position 3808241 upstream of the *waaQ* gene, which is part of the *waa* operon. This operon includes nine other genes, *waaG*, *waaP*, *waaS*, *waaB*, *waaO*, *waaJ*, *waaY*, *waaZ*, and *waaU*, which collectively contribute to lipopolysaccharide (LPS) synthesis[24]. The *waaQ* gene encodes a heptosyltransferase responsible for transferring heptose molecule (III) to the inner core of LPS, which is a critical step in its biosynthesis[33,34].

404 We selected three strains harboring the SNP and three strains without the variant, including
405 the *E. coli* K-12 reference strain. Strains bearing this variant exhibited higher MIC values for
406 TOB (1-8 µg/mL) than those without the variant (0.125–0.5 µg/mL) (**Supplementary Table 8**).
407 To understand the impact of this variant on *waaQ* expression under antibiotic stress, we
408 exposed the strains to ½ MIC for TOB, a sub-inhibitory concentration that is sufficient to induce
409 physiological responses without completely halting bacterial growth. Differential expression
410 analysis of the *waa* operon genes revealed distinct patterns between strains with and without
411 the variant. Two variant-bearing strains (IAI76 and IAI78) showed downregulation of the *waa*
412 operon, whereas one strain (IAI77) displayed incomplete expression of four out of ten *waa*
413 genes (**Figure 8A**). This suggests that the non-coding SNP may influence not only *waaQ*
414 expression, but also the coordinated regulation of other genes in the operon. Gene interaction
415 analysis using the STRING database[35] identified significant links between the *waa* operon
416 genes and known AMR genes *ugd*, and ompF (**Figure 8B**). The *ugd* gene has been tied to LPS
417 modification, resulting in the reduction of antibiotic binding, and uptake[28]. OmpF is a porin that
418 facilitates the diffusion of small hydrophilic molecules across the bacterial membrane, and is
419 frequently associated with reduced antibiotic uptake owing to mutations, as well as being
420 downregulated upon the deletion of *waaF*[28,36,37]. Notably, *ompF* was upregulated in one strain
421 (IAI76), which also exhibited the most pronounced downregulation of the *waa* operon genes.
422 These findings highlight the potential connection between the *waa* operon and AMR pathways
423 involving LPS modification and membrane permeability.

424 We also investigated the SNP, G>T transversion, at position 670,467, upstream of the *murU*
425 gene in *P. aeruginosa*, which was associated with increased resistance to TOB. Six strains
426 were exposed to ½ MIC of TOB for one hour. Strains harboring the *murU* non-coding variant
427 (n=3) exhibited significantly higher TOB resistance (>16 µg/mL) compared to those without
428 this variant (n=3, including the reference strain PA14) (**Supplementary Table 8**). From our
429 differential expression analysis, we did not observe significant changes in *murU* expression
430 between the variant and non-variant strains following TOB exposure.

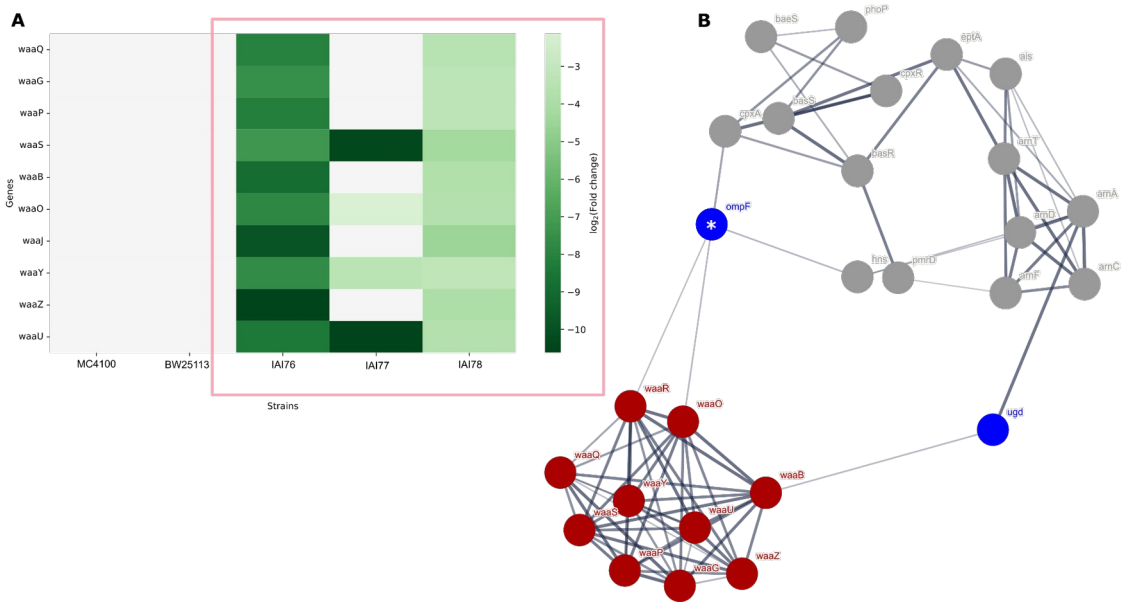

Figure 8: The expression of *waa* operon genes varies per strain with the operon showing connections with known antimicrobial resistant genes in *E. coli*. Six strains (three strains bearing the *waaQ*/3,808,241/T>C variant and three without) were exposed to ½ MIC for TOB for one hour. RNA was extracted after the exposure and sequenced. Transcriptomic analysis was conducted by comparing the expression of genes in each strain with that of the reference strain. **(A)** Expression of the *waa* operon across control and test (red rectangle) strains. A gene was indicated as differentially expressed if it had a log2fold change ≤ -2 or ≥ 2 and an adjusted p-value < 0.0001. **(B)** Interaction between *waa* operon genes (in red) and known antimicrobial-resistant genes (ARGs) (in blue). The asterisk (*) denotes ARGs that are differentially expressed in at least one strain.

Discussion

The ability to use biological sequences alone to determine the characteristics of a living organism has long inspired researchers to identify general rules that would allow for the prediction of phenotypes from primary sequence alone. Fundamentally, this problem can be tackled using two complementary approaches. Mechanistic approaches require a certain level of understanding of the functioning of molecular systems, sometimes down to the level of individual molecules, making its application beyond individual genes or model species prohibitive. In contrast, statistical approaches on the other hand do not require an "intimate" understanding of the system under study, and thus can be applied to a wide variety of molecular processes and species. They do however require a higher upfront "cost" via the accumulation of sufficient observations to achieve an appropriate level of statistical power.

Because of the high coding density of bacterial genomes, the vast majority of genotype-to-phenotype research in this kingdom has focused on predicting the consequences of changes to coding sequences[38]. However, variation in gene expression is likely to be as important in explaining phenotypic changes in bacteria, as exemplified in numerous studies concerning basic physiology[39,40], as well as phenotypes related to infection research[41], such as AMR[42] and pathogenicity[11]. Identifying the extent to which non-coding variants influence gene expression variation could then improve the prediction of phenotype from primary sequence, with positive consequences for diagnostics and synthetic biology.

In this study we have focused on genetic variants in *cis* non-coding regions, under the assumption that in bacterial species they would be responsible for most of the variability in gene expression. We encoded these variants using three distinct data structures, thus ensuring that we would be able to account for all kinds of genetic variations. The use of k-mers in particular, allowed us to jointly consider short variants, gene and promoter presence/absence patterns, and promoter switching, a phenomenon that is estimated to affect up to 16% of DEGs across *E. coli* isolates[9]. We then applied statistical genetics to identify associations between variants and gene expression changes. In the case of *E. coli*, we used the accumulated knowledge on σ^{70} and TFBS sequences to validate the associations mechanistically, as well as experimentally for a smaller subset.

Consistent with the differences in the genetic structure of the two species, we found differences in the proportion of DEGs, for which we identified a variant associated with expression changes. These differences dissipated when using k-mers, for which we found associations for 39% of DEGs in both species, and were only apparent when using short variants and especially promoter switching events. For the latter variant category we could identify associations only for 2% of DEGs in *P. aeruginosa*, as opposed to 28% in *E. coli*. We found the opposite picture when looking at short variants, with associations for 34% of *P. aeruginosa* DEGs, and 7% only for *E. coli*. From these observations we can conclude two things. The first, methodological in nature, confirms that encoding genetic variants as k-mers allows to capture the most genetic variation; the second is that different species have different sources of genetic variation fueling adaptation.

Using external[26] (*E. coli*) and overlapping[10] (*P. aeruginosa*) datasets on susceptibility to antimicrobials, we have shown that non-coding variation is also associated with downstream phenotypes with high clinical relevance. In both species, about one third of the genes with genetic variants (in any region of the genome) associated with drug susceptibility, had these variants encoded in non-coding regions. In *E. coli*, we identified resistance-associated non-coding variants in both known AMR genes such as *gadX*[27] and in genes not previously linked to resistance, such as *waaQ*, a component of the *waa* operon involved in LPS synthesis[24]. Strains with a T>C transition at position 3,808,241 upstream of *waaQ* showed downregulation

489 of the *waa* operon when exposed to sub-inhibitory concentrations of tobramycin. Given the role
490 of LPS in membrane permeability and the observed protein interactions with resistance-related
491 genes *ompF* and *ugd*[28,36], we suggest that this variant may contribute to tobramycin resistance
492 through modification of the outer membrane. For *P. aeruginosa*, we specifically tested the
493 effect of G>T transversion at position 670467, a non-coding variant found in *murU*, a gene
494 involved in peptidoglycan recycling, a mechanism shown to contribute to resistance in the
495 organism[32]. Although we did not observe differential expression of the *murU* gene in variant-
496 bearing strains, the absence of an effect may reflect context-dependent compensatory
497 regulation provided by the strain background or insufficient antibiotic exposure.

498 Even though we have identified a large number of non-coding genetic variants associated with
499 gene expression and AMR, our study has a number of limitations. The limited availability of
500 transcriptomic data reduced the statistical power of our association analyses, especially in *E.*
501 *coli*. Future studies with larger datasets could enhance the robustness of our findings, uncover
502 rarer variants, and associations with more subtle regulatory effects that may have been
503 masked in our study. While collating data from public databases such as ENA and GEO may
504 be a cost-effective way to increase sample size, questions on the homogeneity of experimental
505 and sequencing protocols make this exercise not free from bias. The application of advanced
506 machine learning such as convolutional neural networks[43] (CNNs) and foundation models[44],
507 both able to operate on primary sequence, also holds promise for the identification of genetic
508 variants influencing gene expression. Both would require large datasets for training or even
509 just for validation. Lastly, the lack of well-characterized transcriptional regulatory elements for
510 *P. aeruginosa* prevented the *in-silico* validation of associations in this species. Even for *E. coli*,
511 for which we could make use of the decades of work on characterizing its regulatory network,
512 we could not always validate the associations we identified, which could imply that variants
513 outside of *cis* non-coding regions have a sizable impact on gene expression. Providing a
514 mechanistic model for how those trans variants affect gene regulation will likely be even more
515 difficult.

Methods

Bacterial strains

Whole genome sequences from 117 *E. coli* isolates, and 413 *P. aeruginosa* isolates were obtained from two studies[10,15]. RNA-seq data for *P. aeruginosa* was also obtained from the study from which we obtained the genomes, but for *E. coli*, the data was generated as part of this study. RNA was extracted from exponentially growing bacteria in rich media (LB), with samples being harvested at an OD_{600} of 0.2 (**Supplementary Table 4**). These datasets were analyzed to decipher the relationship between non-coding genetic variants and gene expression in these isolates. For *P. aeruginosa*, data on the susceptibility of each isolate were available for four antibiotics: ciprofloxacin (CIP), gentamicin (GEN), meropenem (MEM), and tobramycin (TOB). We also included an independent dataset[26] of 1,675 *E. coli* isolates together with their susceptibility profiles for 12 antibiotics: Ampicillin (AMP), Cefuroxime (CXM), Cefotaxime (CTX), Cephalothin (CET), Ceftazidime (CTZ), Gentamicin (GEN), Tobramycin (TOB), Ciprofloxacin (CIP), Amoxicillin-clavulanate (AMC), Amoxicillin (AMX), Tazobactam (TZP) and Trimethoprim (TMP). These datasets were used to establish a relationship between non-coding variants and antimicrobial resistance phenotype.

Differential gene expression and functional enrichment analysis

The raw RNA-Seq reads were first assessed for quality using FastQC v0.11.9[45] and aligned to their respective reference genomes (*E. coli* K-12 substr. MG1655, RefSeq accession: NC_000913.3; *P. aeruginosa* UCBPP-PA14, RefSeq accession: NC_008463.1). Transcript quantification was performed using kallisto v0.46.2[46]. Differential gene expression analysis was conducted using DEseq2 v1.44.0[47] for *E. coli* isolates and LPEseq v0.99.5[48] for *P. aeruginosa* isolates, since a single replicate was available for this species. Significance thresholds to identify differentially expressed genes were set as follows: genes needed to be present in at least 10% of isolates to be considered, an adjusted p-value < 0.0001, and an absolute $\log_2$fold change ≥ 2 in at least 5% of the strains. A cluster of orthologous groups (COG) enrichment analysis was performed to highlight the main biological processes influenced by DEGs. Significance was set at an adjusted p-value < 0.05.

Characterization of genetic variants within non-coding regions

Three different genetic markers were used to identify and characterize non-coding genetic variants: short variants (such as SNPs, single nucleotide polymorphisms, InDels, short insertions or deletions), gene cluster specific k-mers, and the presence/absence of intergenic regions (IGRs). For short variants, we performed a whole-genome variant calling analysis using snippy v4.6.0[49] with default parameters, using the reference genome of each species for mapping. We defined a non-coding region as a 230 bp sequence spanning 200 bp upstream from the start codon and 30 bp downstream. Bedtools v2.30.0[50] was used to select short variants occurring only within this 230 bp window. BCFtools v1.13[51] was then used to merge the non-coding variants for each gene across the isolates, which were used as inputs for the association analyses.

A pangenome analysis was conducted for the isolates of both bacterial species using panaroo v1.5.0[52] with default parameters, except for the following arguments: "--clean-mode strict" and "--remove-invalid-genes". We used piggy v1.5[53] to perform a comparative analysis of IGRs across the bacterial isolates. The gene presence/absence matrix generated by panaroo was used as input, and the analysis was performed using default parameters, except for the change in the percentage length identity to 10. We further used the gene presence/absence matrix generated by panaroo to extract gene cluster specific k-mers from the genomic regions flanking each differentially expressed gene using panfeed v1.6.1[14]. The analysis was

563 conducted using the following parameters: "--upstream 200", "--downstream 30", "--no-filter",
564 "--maf 0.1", "--downstream-start-codon", and "--consider missing". The resulting
565 presence/absence from piggy and kmer unique patterns were used as inputs for the
566 association analyses.

567 **Phylogenetic analysis**

568 The phylogenetic tree of the strains was computed using ParSNP v1.2[54], which generated a
569 whole genome nucleotide alignment for all the strains. The resulting tree was visualized using
570 iTOL v6[55].

571 **Associating non-coding variants with gene expression and resistance phenotypes**

572 We performed a GWAS analysis using pyseer v1.3.9[56], to understand the relationship between
573 non-coding genetic variants and gene expression, and antimicrobial resistance phenotypes.
574 For the gene expression phenotype, we examined associations between the presence or
575 absence of non-coding genetic variants (captured by each set of genetic markers) and
576 differentially expressed genes. Variants with minor allele frequencies (MAF) below 10% were
577 excluded from this analysis. Linear mixed models, as implemented in pyseer, were employed
578 to account for genetic relatedness among the isolates, ensuring the robust detection of
579 associations. The population structure was corrected using a similarity matrix generated from
580 the generated phylogenetic tree. To address the issue of multiple testing inherent in GWAS
581 analysis, we applied a pattern-based method that adjusted for the number of unique tests
582 performed. This reduces the risk of over-correcting the association p-values, as it is based on
583 the number of unique tests being carried out. In linking these variants with resistance
584 phenotype, we considered all genes within the bacterial genome, regardless of whether they
585 were differentially expressed. For *E. coli* used a binary phenotype (1-resistance, 0-
586 susceptibility) as the previous authors did, and for *P. aeruginosa* we made use of (MIC) values.
587 This GWAS was conducted in a similar manner as previously described, but with a lower MAF
588 threshold of 0.01 to include rarer variants.

589 **Validating associations between non-coding variants and gene expression in *E.***
590 ***coli***

591 ***In-silico validation***

592 We used a modified version of the Promoter Calculator[13], a biophysical model developed to
593 estimate σ^{70} dependent transcription rates in *E. coli*. We focused on genes where k mers were
594 associated with gene expression, under the hypothesis that these variants might influence
595 transcription by altering the canonical σ^{70} promoter sequence. The predictions were made on
596 230 bp sequences across the strains. The predicted rates were normalised for each gene by
597 dividing the value for each isolate by that of the reference strain, followed by a $\log_2$
598 transformation. A Pearson coefficient was then computed between these values and the
599 corresponding measured gene expression levels across strains. To assess whether these
600 patterns were stronger than expected by chance, we randomly shuffled the predicted rate
601 values 1,000 times across isolates for each gene. A new set of Pearson correlation coefficient
602 was computed between these values and the measured gene expression values. We opted for
603 a global approach to capture broader trends in transcriptional regulation driven by the non-
604 coding variation in promoter regions. This also avoided the burden of multiple testing and
605 variability that may be introduced by per gene analyses. A Kolmogorov–Smirnov test was
606 performed to validate if the observed distribution of correlation coefficients was significantly
607 different from the null distribution. To further validate these associations, We retrieved 93
608 experimentally validated TFBS from RegulonDB[25] and used FIMO[57] to check for the presence

609 of these sites within non-coding sequences. We focused on significant TFBS (adjusted p-value
610 < 0.01, present in at least 10% of the *E. coli* strains). We generated a matrix indicating the
611 presence (1) or absence (0) of TFBS within each gene's non-coding region, which we used to
612 associate with gene expression as previously stated using an MAF of 10%.

613 ***In vitro validation***

614 *Construction of reporter fusion*

615 The pOT2 plasmid (Addgene plasmid #14460) was extracted from 16 hour cultures using a
616 Zyppy plasmid extraction kit (Cat. No. D4019, Zymo Research) following the manufacturer's
617 instructions. The extracted plasmid was linearized using *HindIII* FastDigest restriction enzyme
618 (Cat. No. FD0504, Thermo Fisher Scientific, USA), according to the manufacturer's
619 instructions. The linearized vector was separated from other fragments using 0.7% agarose
620 gel and purified using the Monarch DNA Gel Extraction kit (Cat. No. T1020S; New England
621 Biolabs, UK). The 230bp non-coding regions, as defined above, were amplified using specific
622 primer sets under conditions specified in (**Supplementary Table 5**), and the amplicons were
623 cleaned using Monarch PCR and DNA Clean up Kit (Cat. No. T1030S; New England Biolabs,
624 UK). To generate reporter constructs for each gene, we set up a reaction mixture containing 2
625 µL of 5X In-Fusion Snap Assembly Master Mix (Cat. No. 638951, TaKaRa), 6.6 µL deionized
626 water, and linearized vector and insert at a 1:2 ratio. The mixture was then incubated at 50°C
627 for 15 min in a thermocycler and stored on ice. The assembled product was transformed into
628 chemically competent *E. coli* DH5-alpha cells (Cat. No. 638951; TaKaRa) via heat shock.
629 Transformed cells were plated on LB agar containing 10 µg/mL gentamicin and incubated
630 overnight at 37°C. The following day, colonies were screened by colony PCR using the forward
631 primer of the insert and reverse primer of the vector (**Supplementary Table 2**). Positive clones
632 were sent off for whole plasmid sequencing by Eurofins Scientific to confirm successful
633 cloning.

634 *Measurement of fluorescence in reporter fusions*

635 Each version of the reporter construct (wild-type and mutated) was streaked onto LB agar
636 containing 10 µg/mL gentamicin and incubated overnight at 37°C. Single colonies were grown
637 in 2 mL of freshly prepared M9 medium supplemented with 0.5% glucose, 0.1% casamino
638 acids, 0.01 mg/mL thiamine, 0.123 mg/mL $MgSO_4$, 0.0147 mg/mL $CaCl_2$, 0.0028 mg/mL
639 $FeSO_4.7H_2O$, 10 µg/mL gentamicin. The cultures were incubated overnight at 37°C with
640 shaking at 250 rpm. The next day, cultures were diluted in supplemented M9 media to a final
641 OD_{600} of 0.01 and transferred into black-walled, clear-bottom 96-well plates for growth and
642 fluorescence monitoring. Measurements were taken at a 30-minute interval for 16 h using a
643 Synergy H1 microplate reader with excitation at 395 nm and emission at 509 nm, with each
644 condition tested in triplicate. To assess the effect of non-coding variants on GFP expression,
645 the GFP levels of the mutated reporter constructs were compared to those of their wild-type
646 counterparts. GFP fluorescence measurements beginning at the 6-hour time point were
647 averaged across replicates, normalized to background signal and cell density. The fold change
648 in GFP expression was determined by comparing the mean normalized GFP values of the
649 mutated constructs to those of the wild-type constructs. Cohen's *d* test was applied to compute
650 the effect size and provide the magnitude of differences between the wild-type and mutated
651 reporter constructs.

652 **Antibiotic exposure and RNA extraction**

653 The minimum inhibitory concentration (MIC) of TOB for each bacterial strain was established
654 using the standard microdilution method. Overnight bacterial cultures were diluted at a 1:100
655 dilution factor in Mueller-Hinton (MH) medium and grown to an OD_{600} of 0.6 at 37°C with

656 shaking at 250 rpm. Sub-inhibitory concentrations (½ MIC) of TOB were added to each culture
657 and incubated for an additional hour. Cells were pelleted and treated with RNAprotect (Cat.
658 No. 76506) and stored at -80°C for subsequent extraction using the RNeasy Plus Micro Kit
659 (Qiagen, Cat. No. 76506), according to the manufacturer's instructions. All treatments were
660 performed in duplicate to ensure reproducibility. RNA sequencing was performed by
661 Novogene using the Illumina NovaSeq X Plus platform, producing approximately 2Gb of raw
662 paired reads per sample. The quality of the raw reads was accessed using FastQC v0.11.9[45].
663 The reads were aligned to their respective reference genomes, and transcript quantification
664 and DEG analysis were conducted as described above.

665 **Gene interaction analysis**

666 Protein-protein interaction analysis between *waa* operon and known antimicrobial resistant
667 genes was performed using STRING v12.0[35] web based software. The minimum interaction
668 score was set to 0.4 (moderate confidence), while eliminating text mining as an interaction
669 source. The resulting network was visualized directly through the STRING web interface.

670 **Data availability**

671 The RNA-Seq data generated for the 117 *E. coli* isolates have been deposited in the European
672 Nucleotide Archive (ENA) under accession number PRJNA520928. Transcriptomic data for *E.*
673 *coli* and *P. aeruginosa* isolates exposed to sub-inhibitory concentrations of tobramycin are also
674 available in the ENA under accession number PRJEB83662. Source code for statistical
675 analysis and the generation of figures are available at: https://github.com/microbial-
676 pangenomes-lab/bacterial_transcription

677 **Author contributions**

678 MG conceived the study, with input from BFD, MZ generated the transcriptomic data for *E. coli*
679 with supervision from AT. JE provided support for analyzing the *P. aeruginosa* transcriptomic
680 data under the supervision of SH. BFD analyzed the transcriptomic and genomic data,
681 conducted all the validation experiments, and produced all the figures. BFD and MG wrote the
682 manuscript. All authors provided comments and edits and approved the final version of the
683 manuscript.

684 **Acknowledgments**

685 B.F.D. and M.G. were supported by the Deutsche Forschungsgemeinschaft (DFG, German
686 Research Foundation) under Germany's Excellence Strategy – EXC 2155 (Project No.
687 390874280). B.F.D. were further supported by the Hannover Biomedical Research School
688 (HBRS) and the Centre for Infection Biology (ZIB) and by the Graduate School Scholarship
689 Programme (GSSP) from the German Academic Exchange Service (DAAD). We would like to
690 acknowledge Nick Goldman and Pedro Beltrao from the European Bioinformatics Institute
691 (EMBL-EBI) for their valuable support in generating the transcriptomic data used in this study.

692 **References**

693 1. Lynch M. Streamlining and simplification of microbial genome architecture. Annu Rev
694 Microbiol. 2006;60:327–49.

695 2. Cases I, Lorenzo V de, Ouzounis CA. Transcription regulation and environmental
696 adaptation in bacteria. Trends Microbiol. 2003 Jun 1;11(6):248–53.

697 3. Jacob F, Monod J. Genetic regulatory mechanisms in the synthesis of proteins. J Mol
698 Biol. 1961 Jun 1;3(3):318–56.

699 4. Cotter PA, Miller JF. *In vivo* and *ex vivo* regulation of bacterial virulence gene expression.
700 Curr Opin Microbiol. 1998 Feb 1;1(1):17–26.

701 5. Browning DF, Busby SJW. Local and global regulation of transcription initiation in
702 bacteria. Nat Rev Microbiol. 2016 Oct;14(10):638–50.

703 6. Molina N, Nimwegen E van. Universal patterns of purifying selection at noncoding
704 positions in bacteria. Genome Res. 2008 Jan 1;18(1):148–60.

705 7. Thorpe HA, Bayliss SC, Hurst LD, Feil EJ. Comparative Analyses of Selection Operating
706 on Nontranslated Intergenic Regions of Diverse Bacterial Species. Genetics. 2017 May
707 1;206(1):363–76.

708 8. Yona AH, Alm EJ, Gore J. Random sequences rapidly evolve into de novo promoters. Nat
709 Commun. 2018 Apr 18;9(1):1530.

710 9. Oren Y, Smith MB, Johns NI, Kaplan Zeevi M, Biran D, Ron EZ, et al. Transfer of
711 noncoding DNA drives regulatory rewiring in bacteria. Proc Natl Acad Sci. 2014 Nov
712 11;111(45):16112–7.

713 10. Khaledi A, Weimann A, Schniederjans M, Asgari E, Kuo T, Oliver A, et al. Predicting
714 antimicrobial resistance in Pseudomonas aeruginosa with machine learning-enabled
715 molecular diagnostics. EMBO Mol Med. 2020 Mar 6;12(3):e10264.

716 11. Earle SG, Lobanovska M, Lavender H, Tang C, Exley RM, Ramos-Sevillano E, et al.
717 Genome-wide association studies reveal the role of polymorphisms affecting factor H
718 binding protein expression in host invasion by Neisseria meningitidis. PLoS Pathog. 2021
719 Oct;17(10):e1009992.

720 12. Urtecho G, Insigne KD, Tripp AD, Brinck MS, Lubock NB, Acree C, et al. Genome-wide
721 Functional Characterization of Escherichia coli Promoters and Sequence Elements
722 Encoding Their Regulation. eLife [Internet]. 2023 Dec 12 [cited 2025 May 17];12.
723 Available from: https://elifesciences.org/reviewed-preprints/92558

724 13. LaFleur TL, Hossain A, Salis HM. Automated model-predictive design of synthetic
725 promoters to control transcriptional profiles in bacteria. Nat Commun. 2022 Sep
726 2;13(1):5159.

727 14. Sommer H, Djamalova D, Galardini M. Reduced ambiguity and improved interpretability
728 of bacterial genome-wide associations using gene-cluster-centric k-mers. Microb
729 Genomics. 2023;9(11):001129.

15. Galardini M, Koumoutsi A, Herrera-Dominguez L, Cordero Varela JA, Telzerow A, Wagih O, et al. Phenotype inference in an Escherichia coli strain panel. eLife. 2017 Dec 27;6:e31035.

16. Avalos Vizcarra I, Hosseini V, Kollmannsberger P, Meier S, Weber SS, Arnoldini M, et al. How type 1 fimbriae help Escherichia coli to evade extracellular antibiotics. Sci Rep. 2016 Jan 5;6(1):18109.

17. Jang S. AcrAB−TolC, a major efflux pump in Gram negative bacteria: toward understanding its operation mechanism. BMB Rep. 2023 Jun 30;56(6):326–34.

18. The UniProt Consortium. UniProt: the Universal Protein Knowledgebase in 2025. Nucleic Acids Res. 2025 Jan 6;53(D1):D609–17.

19. Winsor GL, Griffiths EJ, Lo R, Dhillon BK, Shay JA, Brinkman FSL. Enhanced annotations and features for comparing thousands of Pseudomonas genomes in the Pseudomonas genome database. Nucleic Acids Res. 2016 Jan 4;44(Database issue):D646–53.

20. Le Mauff F, Razvi E, Reichhardt C, Sivarajah P, Parsek MR, Howell PL, et al. The Pel polysaccharide is predominantly composed of a dimeric repeat of α-1,4 linked galactosamine and N-acetylgalactosamine. Commun Biol. 2022 May 26;5(1):1–7.

21. Bouteiller M, Dupont C, Bourigault Y, Latour X, Barbey C, Konto-Ghiorghi Y, et al. Pseudomonas Flagella: Generalities and Specificities. Int J Mol Sci. 2021 Mar 24;22(7):3337.

22. Lorusso AB, Carrara JA, Barroso CDN, Tuon FF, Faoro H. Role of Efflux Pumps on Antimicrobial Resistance in Pseudomonas aeruginosa. Int J Mol Sci. 2022 Jan;23(24):15779.

23. Gold VA, Salzer R, Averhoff B, Kühlbrandt W. Structure of a type IV pilus machinery in the open and closed state. Harrison SC, editor. eLife. 2015 May 21;4:e07380.

24. Karp PD, Paley S, Caspi R, Kothari A, Krummenacker M, Midford PE, et al. The EcoCyc Database (2023). EcoSal Plus. 2023 May 11;11(1):eesp-0002-2023.

25. Salgado H, Gama-Castro S, Peralta-Gil M, Díaz-Peredo E, Sánchez-Solano F, Santos-Zavaleta A, et al. RegulonDB (version 5.0): Escherichia coli K-12 transcriptional regulatory network, operon organization, and growth conditions. Nucleic Acids Res. 2006 Jan 1;34(suppl_1):D394–7.

26. Moradigaravand D, Palm M, Farewell A, Mustonen V, Warringer J, Parts L. Prediction of antibiotic resistance in Escherichia coli from large-scale pan-genome data. PLOS Comput Biol. 2018 Dec 14;14(12):e1006258.

27. Nishino K, Senda Y, Yamaguchi A, Nishino K, Yamaguchi A, Nishino K, et al. The AraC-family regulator GadX enhances multidrug resistance in *Escherichia coli* by activating expression of *mdtEF* multidrug efflux genes. J Infect Chemother. 2008 Jan 1;14(1):23–9.

28. Alcock BP, Huynh W, Chalil R, Smith KW, Raphenya AR, Wlodarski MA, et al. CARD 2023: expanded curation, support for machine learning, and resistome prediction at the Comprehensive Antibiotic Resistance Database. Nucleic Acids Res. 2023 Jan

770 6;51(D1):D690–9.

771 29. Sukhodolets MV, Garges S, Adhya S. Ribosomal protein S1 promotes transcriptional
772 cycling. RNA. 2006 Aug 1;12(8):1505–13.

773 30. Kitakawa M, Isono K. An amber mutation in the gene rpsA for ribosomal protein S1 in
774 Escherichia coli. Mol Gen Genet MGG. 1982 May 1;185(3):445–7.

775 31. Vallejos-Sánchez K, Lopez JM, Antiparra R, Toscano E, Saavedra H, Kirwan DE, et al.
776 Mycobacterium tuberculosis ribosomal protein S1 (RpsA) and variants with truncated C-
777 terminal end show absence of interaction with pyrazinoic acid. Sci Rep. 2020 May
778 20;10(1):8356.

779 32. Fumeaux C, Bernhardt TG. Identification of MupP as a New Peptidoglycan Recycling
780 Factor and Antibiotic Resistance Determinant in Pseudomonas aeruginosa. mBio. 2017
781 Mar 28;8(2):e00102-17.

782 33. Yethon JA, Heinrichs DE, Monteiro MA, Perry MB, Whitfield C. Involvement of waaY,
783 waaQ, and waaP in the Modification of Escherichia coliLipopolysaccharide and Their
784 Role in the Formation of a Stable Outer Membrane *. J Biol Chem. 1998 Oct
785 9;273(41):26310–6.

786 34. Mudapaka J, Taylor EA. Cloning and characterization of the Escherichia coli
787 Heptosyltransferase III: Exploring substrate specificity in lipopolysaccharide core
788 biosynthesis. FEBS Lett. 2015 Jun 4;589(13):1423–9.

789 35. Szklarczyk D, Kirsch R, Koutrouli M, Nastou K, Mehryary F, Hachilif R, et al. The STRING
790 database in 2023: protein–protein association networks and functional enrichment
791 analyses for any sequenced genome of interest. Nucleic Acids Res. 2023 Jan
792 6;51(D1):D638–46.

793 36. Simonet V, Malléa M, Pagès JM. Substitutions in the Eyelet Region Disrupt Cefepime
794 Diffusion through the Escherichia coli OmpF Channel. Antimicrob Agents Chemother.
795 2000 Feb;44(2):311–5.

796 37. Sakenova N, Cacace E, Orakov A, Huber F, Varik V, Kritikos G, et al. Systematic
797 mapping of antibiotic cross-resistance and collateral sensitivity with chemical genetics.
798 Nat Microbiol. 2025 Jan;10(1):202–16.

799 38. Wagih O, Galardini M, Busby BP, Memon D, Typas A, Beltrao P. A resource of variant
800 effect predictions of single nucleotide variants in model organisms. Mol Syst Biol. 2018
801 Dec;14(12):e8430.

802 39. Wolf L, Silander OK, van Nimwegen E. Expression noise facilitates the evolution of gene
803 regulation. Golding I, editor. eLife. 2015 Jun 17;4:e05856.

804 40. Julou T, Gervais T, de Groot D, van Nimwegen E. Growth rate controls the sensitivity of
805 gene regulatory circuits. Sci Adv. 2025 Apr 25;11(17):eadu9279.

806 41. Barczak AK, Gomez JE, Kaufmann BB, Hinson ER, Cosimi L, Borowsky ML, et al. RNA
807 signatures allow rapid identification of pathogens and antibiotic susceptibilities. Proc Natl
808 Acad Sci. 2012 Apr 17;109(16):6217–22.

42. Khaledi A, Schniederjans M, Pohl S, Rainer R, Bodenhofer U, Xia B, et al. Transcriptome Profiling of Antimicrobial Resistance in Pseudomonas aeruginosa. Antimicrob Agents Chemother. 2016 Jul 22;60(8):4722–33.

43. Barbadilla-Martínez L, Klaassen N, van Steensel B, de Ridder J. Predicting gene expression from DNA sequence using deep learning models. Nat Rev Genet. 2025 May 13;1–15.

44. Nguyen E, Poli M, Durrant MG, Kang B, Katrekar D, Li DB, et al. Sequence modeling and design from molecular to genome scale with Evo. Science. 2024 Nov 15;386(6723):eado9336.

45. Andrews S. s-andrews/FastQC [Internet]. 2024 [cited 2024 Aug 28]. Available from: https://github.com/s-andrews/FastQC

46. Bray NL, Pimentel H, Melsted P, Pachter L. Near-optimal probabilistic RNA-seq quantification. Nat Biotechnol. 2016 May;34(5):525–7.

47. Love MI, Huber W, Anders S. Moderated estimation of fold change and dispersion for RNA-seq data with DESeq2. Genome Biol. 2014 Dec 5;15(12):550.

48. Gim J, Won S, Park T. LPEseq: Local-Pooled-Error Test for RNA Sequencing Experiments with a Small Number of Replicates. PLOS ONE. 2016 Aug 17;11(8):e0159182.

49. Seemann T. tseemann/snippy [Internet]. 2024 [cited 2024 Aug 28]. Available from: https://github.com/tseemann/snippy

50. Quinlan AR, Hall IM. BEDTools: a flexible suite of utilities for comparing genomic features. Bioinformatics. 2010 Mar 15;26(6):841–2.

51. Narasimhan V, Danecek P, Scally A, Xue Y, Tyler-Smith C, Durbin R. BCFtools/RoH: a hidden Markov model approach for detecting autozygosity from next-generation sequencing data. Bioinformatics. 2016 Jun 1;32(11):1749–51.

52. Tonkin-Hill G, MacAlasdair N, Ruis C, Weimann A, Horesh G, Lees JA, et al. Producing polished prokaryotic pangenomes with the Panaroo pipeline. Genome Biol. 2020 Jul 22;21(1):180.

53. Thorpe HA, Bayliss SC, Sheppard SK, Feil EJ. Piggy: a rapid, large-scale pan-genome analysis tool for intergenic regions in bacteria. GigaScience. 2018 Apr 1;7(4):giy015.

54. Treangen TJ, Ondov BD, Koren S, Phillippy AM. The Harvest suite for rapid core-genome alignment and visualization of thousands of intraspecific microbial genomes. Genome Biol. 2014 Nov 19;15(11):524.

55. Letunic I, Bork P. Interactive Tree of Life (iTOL) v6: recent updates to the phylogenetic tree display and annotation tool. Nucleic Acids Res. 2024 Jul 5;52(W1):W78–82.

56. Lees JA, Galardini M, Bentley SD, Weiser JN, Corander J. pyseer: a comprehensive tool for microbial pangenome-wide association studies. Bioinformatics. 2018 Dec 15;34(24):4310–2.

847 57. Grant CE, Bailey TL, Noble WS. FIMO: scanning for occurrences of a given motif.
848 Bioinformatics. 2011 Apr 1;27(7):1017–8.